NANO LETTERS

pubs.acs.org/NanoLett

Micro- and Nanopatterning of Inorganic and Polymeric Substrates by Indentation Lithography

Jinlong Gong,[†] Darren J. Lipomi,[†] Jiangdong Deng,[‡] Zhihong Nie,[†] Xin Chen,[†] Nicholas X. Randall,[§] Rahul Nair,[§] and George M. Whitesides[†,*]

[†]Department of Chemistry and Chemical Biology, Harvard University, 12 Oxford Street, Cambridge, Massachusetts 02138, [‡]Center for Nanoscale Systems, Harvard University, 9 Oxford Street, Cambridge, Massachusetts 02138, and [§]CSM Instruments Inc., 197 First Avenue, Suite 120, Needham, Massachusetts 02494

ABSTRACT This paper describes the use of a nanoindenter, equipped with a diamond tip, to form patterns of indentations on planar substrates (epoxy, silicon, and SiO_2). The process is called "Indentation Lithography" (IndL). The indentations have the form of pits and furrows, whose cross-sectional profiles are determined by the shapes of the diamond indenters, and whose dimensions are determined by the applied load and hardness of the substrate. IndL makes it possible to indent hard materials, to produce patterns with multiple levels of relief by changing the loading force, and to control the profiles of the indentations by using indenters with different shapes. This paper also demonstrates the transfer of indented patterns to elastomeric PDMS stamps for soft lithography, and to thin films of evaporated gold or silver. Stripping an evaporated film from an indented template produces patterns of gold or silver pyramids, whose tips concentrate electric fields. Patterns produced by IndL can thus be used as substrates for surface-enhanced Raman scattering (SERS) and for other plasmonic applications.

KEYWORDS Nanoindentation, surface patterning, lithography, SERS, nanofabrication

This paper describes the use of a commercial nanoindenter to generate topographic patterns on substrates such as epoxy, silicon, and SiO_2. We call the process "Indentation Lithography" and abbreviate it as IndL. The patterns comprise features of indentations and furrows with well-defined sidewalls and dimensions and are created using a diamond indenter, controlled using commercial software. This process is a new method for fabricating patterns of micro- and nanoscale features for soft lithography. It has four characteristics not found in other techniques (e.g., electron-beam lithography (EBL) and photolithography) used to fabricate patterns of nanostructures.[1] (i) It can generate multiple levels of relief (different values of height) easily by changing the loading force. (ii) It can control the profiles of the indentations by using indenters with different shapes. (iii) It can indent hard materials (thermally grown SiO_2, glass, and metals) because it uses a diamond tip. (iv) It can produce features with a wide range of depths (e.g., from a few to several hundred nanometers). These characteristics combine to produce patterns with three-dimensional relief in hard materials; this type of typography has not been exploited and is difficult or impossible to achieve using lithographic techniques in which features in resist can have only one value of height and approximately vertical sidewalls. The technique does not require chemical processing and proceeds in an ambient environment. Nanoindentation is a versatile and ubiquitous tool for metrology,[2] but has not been previously explored as a lithographic tool (aside from conceptually related, but practically very different, scanning probe-based techniques[3]).

Background. "Nanofabrication" is, in principle, any process that generates patterns of structures with sizes less than 100 nm in at least one dimension. Scanning-beam techniques, such as EBL and focused-ion-beam (FIB) writing, are the principal methods of generating arbitrary nanoscale patterns (mastering); photolithography is the principal method of transferring these patterns from one substrate to another (replication).[4,5] These techniques, while the workhorses of nanofabrication, come with high capital and operating costs, limited accessibility to general users (and users of materials considered incompatible with electronics fabrication). Photolithography and EBL are generally only applicable to the two-dimensional patterning of resist materials on planar substrates.[4]

Soft lithography is a collection of techniques that transfers patterns by printing or molding using an elastomeric stamp.[4,6−9] Fabricating these stamps involves casting and curing a prepolymer (typically polydimethylsiloxane, PDMS) against a rigid master presenting topographic features. The cured stamp is an inverse replica of the master. A large number of techniques have successfully generated masters for soft lithography,[6,10] and this technique owes much of its utility in patterning on the microscale to the use of inexpensive, printed transparency masks combined with photoli-

*To whom correspondence should be addressed. E-mail: gwhitesides@gmwgroup.harvard.edu.

Received for review: 05/11/2010
Published on Web: 06/17/2010

DOI: 10.1021/nl101675s | *Nano Lett.* **2010,** *10,* 2702–2708

thography.[11] Generating patterns with submicrometer features, however, is more challenging. The most common method of generating masters with arbitrary nanoscale patterns is scanning-beam lithography (EBL, FIB, and direct laser writing).[9,12] A simple alternative of producing surface patterns with nanoscale features would expand the capabilities of soft lithography for nanopatterning.

Nanoindentation is a technique normally used to measure the mechanical properties (e.g., hardness and elastic modulus) of materials, thin films, and coatings.[2,13] Modern nanoindentation systems equipped with diamond-tipped indenters are precise instruments that, when equipped with suitable software, are capable of producing indentations and furrows in a variety of geometries. The shapes of the features depend on the shapes of the probe tips used. Indentation systems, equipped with a diamond indenter, can indent essentially any material. With routine use of approximately one hundred indentations per day on polymeric samples, the lifetime of a tip is about two years. Indenting metallic or ceramic substrates dulls a tip more quickly than indenting soft materials, but a tip still retains its sharpness for several months with routine usage. A precision nanoindentation system with a programmable x, y stage costs ~$150 K (2010), and while expensive, it is less expensive than an FIB system or e-beam writer.

Figure 1a depicts the use of nanoindentation as a tool for micro- and nanofabrication and summarizes the procedure used to transfer the patterns to elastomeric stamps, which in turn can be used to pattern other materials. We also used indented silicon dioxide (thermally grown on Si(110) substrates) as templates for an evaporated gold or silver film, which can be "template stripped" (Figure 1b).[14] This action produced smooth metallic films with pyramidal structures that can be used to concentrate electric fields. These structures can thus be used as substrates for SERS and for other plasmonic applications.

Comparison of IndL with Scanning-Probe Lithography. The use of a diamond probe for lithography has many conceptual similarities to scanning probe lithography (SPL, which uses, for example, an atomic force microscope, AFM[15−20]), and other techniques, such as dip-pen nanolithography,[16] nanoshaving, and nanografting.[17] These techniques use a probe whose position can be scanned relative to a substrate to write a pattern. There are, however, four important differences between IndL and SPL. (i) IndL can be used to pattern hard materials, because it uses a diamond tip that is driven vertically into the substrate. IndL is thus capable of greater applied loads than is SPL, which relies on a cantilever, and is limited to patterning relatively soft materials (e.g., polymers). (ii) IndL can generate structures with a greater range of different widths and depths than can SPL, because IndL is capable of applying loads over several orders of magnitudes (100 nN − 1 N). AFM lithography, for example, can only produce shallow structures, since it can only apply relatively small forces (typically 1 pN − 10 μN). Higher loading forces could damage or reduce the lifetime of the cantilever.[21] (iii) IndL has a large working window (10 cm × 10 cm) over which it can pattern without stitching. (iv) IndL can produce three-dimensional indented features by using probes with different shapes.

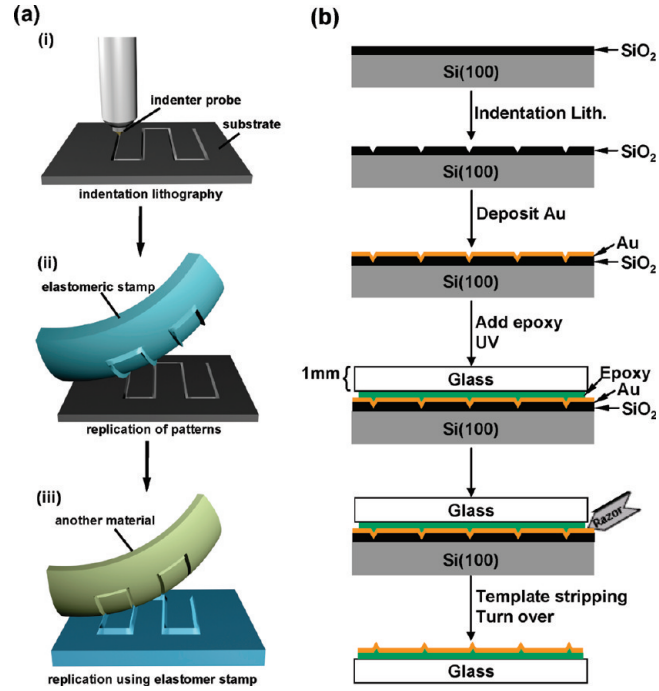

FIGURE 1. (a) Diagram summarizing the method for patterning substrates using Indentation Lithography. (i) The diamond indenter generates patterns by either scratching or pressing into the surface. (ii) These patterns are replicated by pouring an elastomeric prepolymer over the patterned substrate. Curing and separating the elastomer generates a stamp bearing relief features; this stamp is an inverse replica of the original pattern. (iii) The elastomeric stamp, in turn, can be used to template replicas of the original pattern in other materials (e.g., epoxy). (b) Schematic diagram of the procedure for template stripping of metal films using the composite of glass/epoxy as a mechanical support.

IndL employed in this work has lower resolution and less accuracy (~100 nm) in positioning than SPL (~1 nm). This accuracy, however, does not depend on fundamental limitations, but on the accuracy of the system built for metrology, which does not require single-nanometer accuracy. We expect that a system for nanoindentation designed for lithography could be engineered to approach the accuracy of SPL (e.g., use of a higher-resolution sample displacement stage).

Experimental Design. ***Nanoindentation Systems.*** We used a CSM Instruments Open Platform equipped with two dedicated modules: a CSM Instruments Ultra Nanoindentation Tester (UNHT) mounted with a Berkovich indenter (symmetrical pyramid, total included angle 142.35°) was used for making 2D arrays of nanoindentations; a CSM Instruments Nano Scratch Tester (NST) mounted with a 1 μm radius conical diamond indenter was used for continuous scratching of the surface. Accurate sample

DOI: 10.1021/nl101675s | *Nano Lett.* **2010,** *10,* 2702–2708

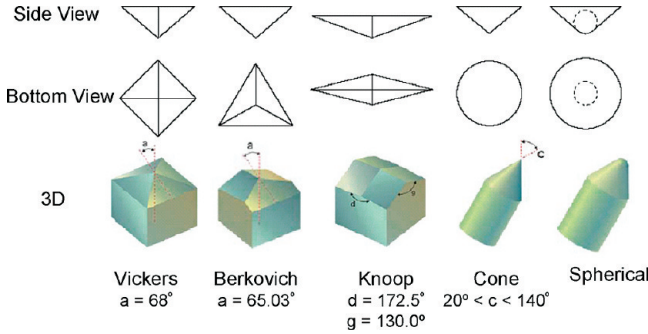

FIGURE 2. Schematic illustration of several types of standard indenter probes. These probes can be selected based on requirements of the application.

displacement was achieved with a Physik Instrumente (PI) P-733.2CD stage to pattern furrows and split rings. We chose these indentation/scratch systems because they are controlled by software that allows easy programming of patterns of indentations and furrows. Berkovich and conical probes are two of the most common, commercially available diamond tips (Figure 2). An integrated AFM system allowed immediate imaging of the nanoindentations or scratches without having to search for them in a separate system.

Substrates. We used three substrates, a 1 μm thick silica film thermally grown on a Si(100) wafer, a Si(100) wafer bearing a native layer of SiO_2 (~2.5 nm), and a flat epoxy substrate generated by puddle-casting an epoxy prepolymer against the polished surface of a Si(100) wafer. The mechanical properties (e.g., hardness, elastic modulus) of the materials determine the extent of "sink-in" or "pile-up" around the peripheries of the indentations.[13] We chose thermally grown SiO_2 because it produced negligible pile-up.

Patterns. We chose three patterns, (i) a square array of indentations with either uniform size (as a matter of replication for SERS substrates) or two different layers of relief, "large" (deep and wide) and "small" (shallow and narrow), in the shape of inverted trigonal pyramids; (ii) straight parallel furrows connected at the ends by right angles to demonstrate the fabrication of channels with constant depth (with a potential application of making microfluidic devices); and (iii) a rectangular array of split rings to demonstrate the ability to make curved features. We chose 2D arrays of split rings to demonstrate the ability to produce curved lines, and because concentric split ring structures have interesting and useful plasmonic properties.[22]

Molding. We replicated the topographic patterns produced by indentation lithography in PDMS, gold, and silver. The choice of PDMS allowed us to demonstrate the ability to produce stamps whose features retained the dimensions and sharpness of the template. We also replicated a square array of indented features using template stripping[14] to obtain ultrasmooth pure metallic films with pyramidal structures that served as substrates for surface-enhanced Raman scattering.

Results and Discussion. ***Fabrication of a 2D Array of Indentations.*** IndL makes it relatively easy to produce patterns with multiple levels of relief, by using different applied loads on the same substrate to change the depth of penetration. Figure 3a shows a schematic drawing of a pattern of trigonal pyramidal indentations that were produced in a 1 μm thick film of SiO_2. We generated two sizes of indentations with the same shape. These indentations differed by an order of magnitude in width and depth. Figure 3b is a three-dimensional AFM image of a 3 × 3 array of indentations in a SiO_2 film that alternated between large and small indentations. Figure 3c shows a close-up 2D AFM image of a 2 × 2 array of indentations. We obtained a profile of the depths of a large and a small indentation in the pattern (Figure 3d) across the red line shown in Figure 3c. The measurements showed the reproducibility of the features. Large indentations were 920 ± 13 nm ($N = 5$) in width and 110 ± 3 nm in depth; small indentations were 190 ± 3 nm ($N = 4$) in width and 11 ± 0.5 nm in depth. The spacing between indentations was 3.5 μm. The resolution of the displacement stage of the system determined the minimum achievable distance between indentations (~100 nm).

Fabrication of Channels. Figure 4a is a schematic diagram of a pattern of channels we scratched into epoxy. The pattern consisted of parallel channels with length of 70 μm and spacing of 5 μm, connected at the ends to form a single, unbroken channel. Figure 4 panels b and c are AFM images of portions of the channels in epoxy. These channels accurately reproduced the geometry of the desired pattern. The 1 μm radius conical diamond indenter produced grooves with shallow V-shaped profiles (Figures 4d). Line scans perpendicular to the channels yielded an average depth of 77 ± 12 nm ($N = 8$). The average height of pile-up was 40 ± 6 nm ($N = 8$). The shape, depth, and width of channels depended on the loading force and the shape of the indenter probe. We did not observe any elastic recovery of the indentations, suggesting that the diamond indenter deformed the substrate permanently. The same loading force (250 μN) left a shallower scratch (not shown) in Si(100) (~3 nm) than it did in epoxy (~ 75 nm), because silicon is much harder than epoxy.

The line width of a scratch is a function of both the contact force and the sharpness of the indenter. The instruments we used were capable of extremely low contact forces (≥10 μN), which are generally not high enough to permanently deform hard substrates (e.g., SiO_2, TiO_2, and carbides). The minimum line width, therefore, depended strongly on the sharpness of the probe and on the hardness of the material.

Fabrication of 2D Array of Split Rings. We designed the split rings shown in Figure 5a in order to demonstrate that IndL can be used to generate curved structures. The

DOI: 10.1021/nl101675s | *Nano Lett.* **2010,** *10,* 2702–2708

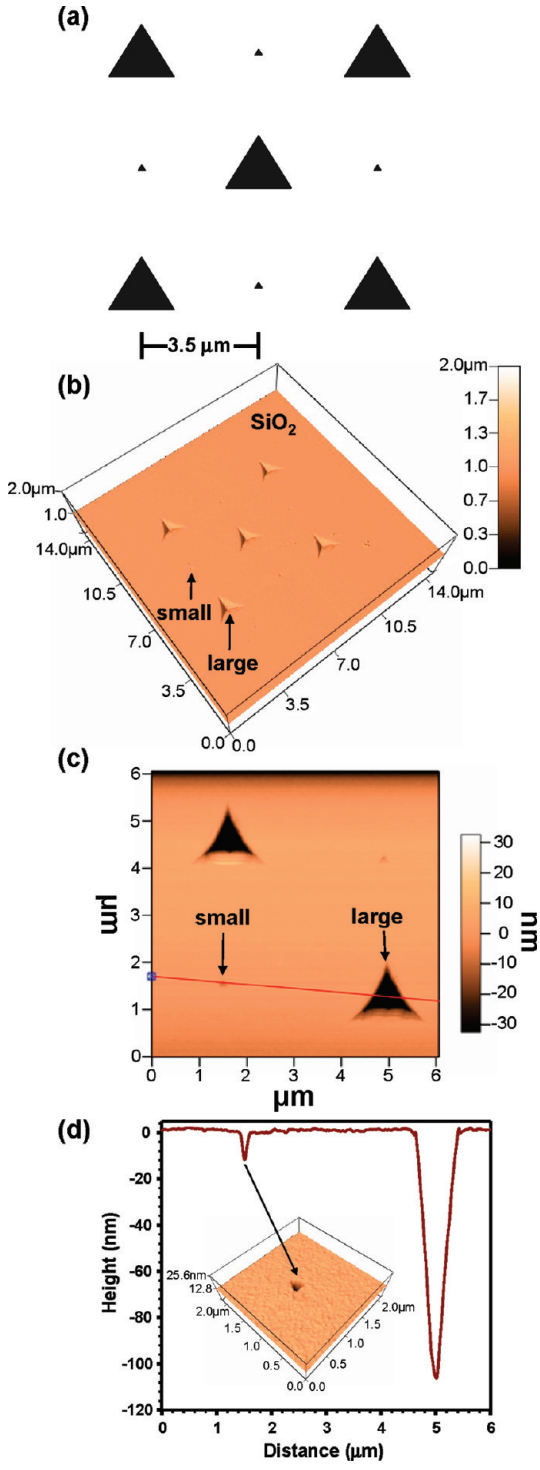

FIGURE 3. (a) Schematic drawing of a 2D array with alternating large and small indentations separated by 3.5 μm and produced by applying two different loading forces. (b) Three-dimensional AFM image of the 3 × 3 array of indentations patterned on a silica film (1 μm thick) grown on Si(100). (c) An expanded 2D AFM image of 2 × 2 array of indentations. (d) Two-dimensional line profile along x-direction marked with the red line in image (c). The inset is a high-resolution AFM image of a small indentation. The loading forces used for large and small indentations were 0.5 and 10 mN, respectively. The width of a large indentation is 920 ± 13 nm (N = 5) and the depth is 110 ± 3 nm. The small indentations are 190 ± 3 nm (N = 4) in width and 11 ± 0.5 nm in depth.

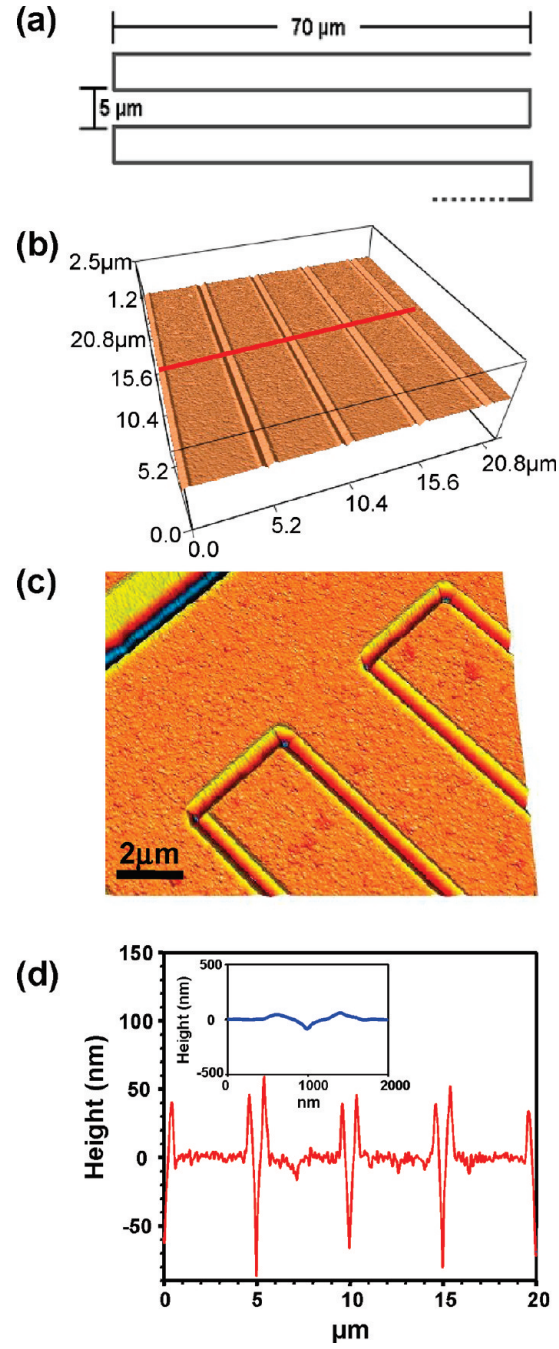

FIGURE 4. (a) Schematic drawing of channels with 70 μm length and 5 μm between each channel. (b) The 3D AFM images of a portion of the channels on epoxy. (c) A close-up 2D AFM image of the ends of the channels, which are connected by orthogonal line segments, on epoxy. (d) Two-dimensional line profile (note that x and y axes are not in the same scale) along the red line drawn on image (b). The inset is a profile of a single channel with the x- and y-axes rescaled to illustrate the shape of the profile.

rings had an outer diameter of 10 μm, a line width of 350 nm, and an opening of 60°. The pitch of these rings within the array was 20 μm. Figure 5 panels b and c are optical and AFM images of split rings scratched into a silicon wafer. This pattern reproduced the geometry that we input into the software that controlled the stage. Depth profiles from the

DOI: 10.1021/nl101675s | Nano Lett. 2010, 10, 2702–2708

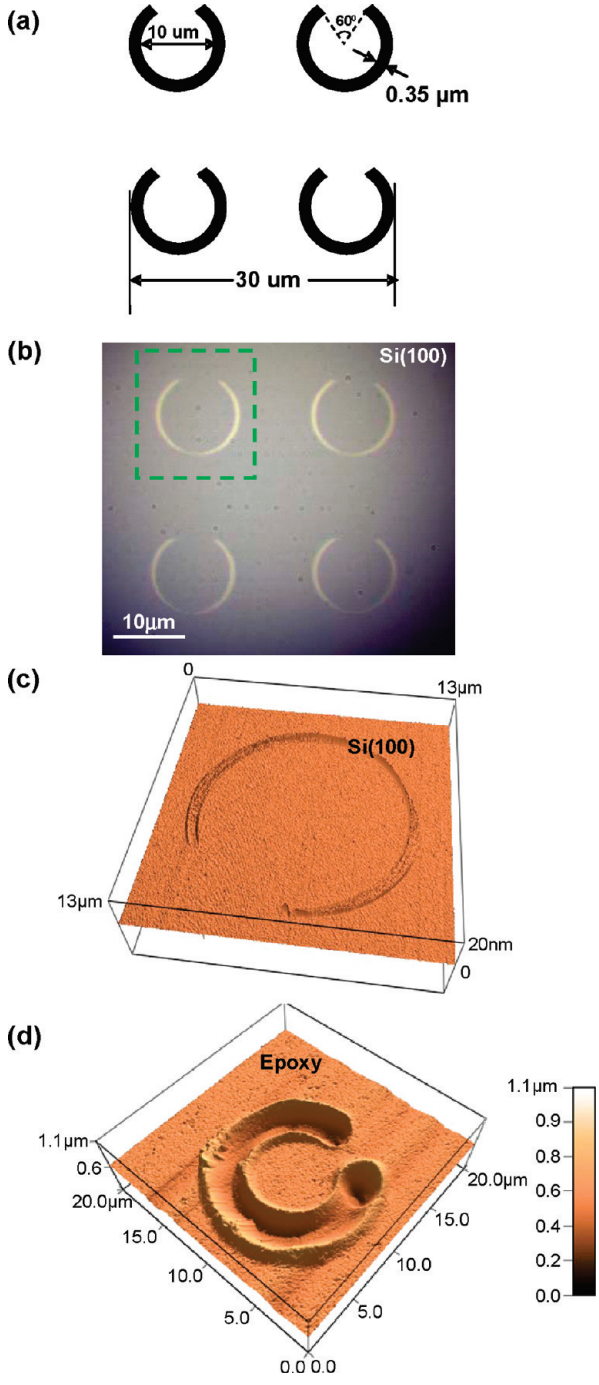

FIGURE 5. (a) Schematic drawing of a 2D array of split rings with an outer diameter of 10 μm, a line width of 350 nm, and a 60° opening. The center-to-center distance between rings is 20 μm. (b) Optical and (c) 3D AFM images of 2D array of split rings on silicon. (d) 3D AFM image of a split ring on epoxy.

AFM image (Figure 5c) indicated that the depth of these rings was 2.0 ± 0.4 nm. The average height of pile-up was 2.3 nm. We also successfully fabricated a 2D array of split rings on an epoxy substrate; Figure 5d is a three-dimensional AFM image of a single feature.

Pile-Up. Indentation of some materials (e.g., epoxy and Si, but not a 1 μm thick layer of thermally grown SiO_2 on a Si(110) substrate) produced "pile-up" of material displaced by plastic deformation around the perimeter of the indentations. We were unable to remove piled-up material by blowing with a stream of compressed nitrogen, stripping it with adhesive tape, or sonicating it in acetone. The strength of adhesion of the pile-up to the substrate suggested that it was either plastically deformed material or fragmented particles attached strongly to the substrate. Generation of pile-up depends on intrinsic material properties, such as the ratio of the effective modulus to the yield stress (E_{eff}/σ_y), and the work-hardening behavior.[23] In general, pile-up is significant in materials with large values of E_{eff}/σ_y (e.g., materials that show rigid-plastic behavior) and little or no capacity for work hardening (i.e., "soft" metals that have been cold-worked prior to indentation). The capacity for work hardening inhibits pile-up because, as material at the surface adjacent to the indenter hardens during deformation, it constrains the upward flow of material to the surface. For example, ceramics, silica, and cold-worked hard metals generate negligible pile-up.[23]

Profile of Structures. In IndL, the profile (e.g., shape and aspect ratio of depth and width) of structures is predefined by the geometry of the indenter probe. There are several types of standard probes, which can be divided into the following three groups: three-sided, four-sided, and conical (Figure 2). The probe can, also, be customized based on the application.

Generation of Elastomeric Stamps from Patterned Substrates. Elastomeric stamps can reproduce nanoscale features with high fidelity. For example, Xu at al. showed that it was possible to replicate a crack in a silicon wafer with PDMS with resolution of 0.4 nm.[24] To show that patterns of silicon generated in the SiO_2 film could be transferred to PDMS, we poured a PDMS prepolymer over the SiO_2 substrate. Thermal curing provided an inverse replica with relief features whose dimensions were indistinguishable from those on the substrate. Figure 6a is a three-dimensional AFM image of the PDMS replica bearing a 3 × 3 grid of large and small pyramids. We made these structures by casting the PDMS prepolymer against the recessed features indented in SiO_2 shown in Figure 3. Figure 6b is a close-up topographic image of a small indentation marked by a green oval in Figure 6a. Figure 6c is a line profile of a large and small indentation corresponding to the red line in Figure 6a. Comparison of the line profiles in Figure 3d and Figure 6c indicates that the heights and widths of the raised features are the same as the depths and widths of the recessed features of the SiO_2 master.

Generation of Ultrasmooth Pure Metal Films with Pyramidal Structures. After the wafer was patterned with indentation lithography, we coated it with a thin film of silver or gold using e-beam evaporation, followed by a layer of epoxy, by puddle-casting and UV-curing a prepolymer.[14,25] We then peeled off the epoxy-metal bilayer to reveal a patterned metallic film whose surface roughness between

DOI: 10.1021/nl101675s | Nano Lett. 2010, 10, 2702–2708

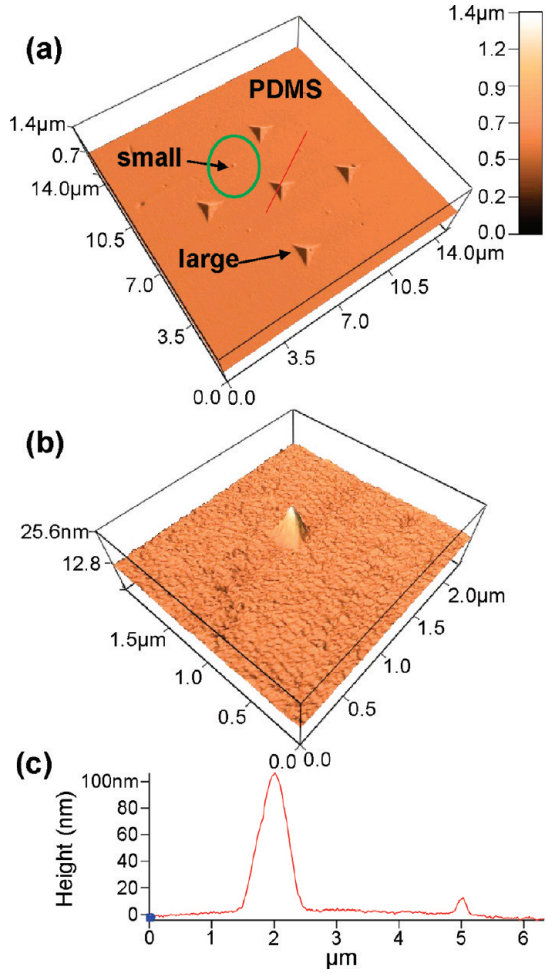

FIGURE 6. AFM images of PDMS stamps templated by the SiO_2 substrate shown in Figure 3. (a) A 3D image of an inverse replica of the array. (b) A close-up 3D image of a small indentation marked by a green oval in (a). (c) One-dimensional line profile of a large and small indentation corresponding to the red line in (a).

features was determined by the wafer template (Figure 1b). Figure 7a shows a SiO_2/Si(100) (1 μm thick silica film thermally grown in Si(100)) substrate patterned with 5 × 5 array of indentations (using a loading force of 20 mN). We evaporated 100 nm of silver on this substrate, added epoxy, and peeled off the bilayer. Figure 7b,c shows the smooth silver film with raised pyramidal structures that was peeled off from this wafer. Comparison of Figure 7 panels a and b suggests the high quality of the process.

Pyramidal Structures for Surface-Enhanced Raman Scattering. Gold and silver films have been investigated for enhanced molecular and biological sensing due to the concentrated electric fields near patterned metallic nanostructures.[26,27] The ability to generate enhancements with films that are easily and reproducibly fabricated is a current challenge in fabrication for plasmonics.[25] We formed a self-assembled monolayer (SAM) of 4-methylbenzenethiol to this silver surface (shown in Figure 7b,c) and used scanning confocal Raman microscopy to collect the SERS signal as a function of position. The resulting image for scans revealed

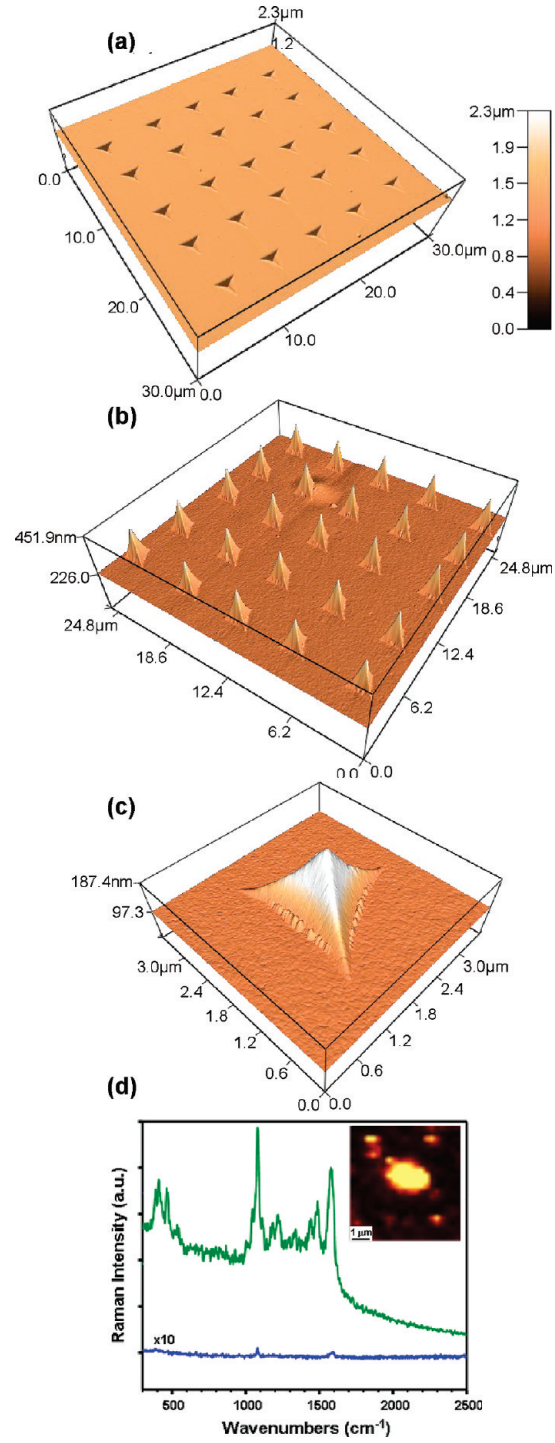

FIGURE 7. (a) AFM image of a 100 μm thick film of thermally grown SiO_2 on a Si(100) wafer patterned with a 5 × 5 array of indentations separated by 5 μm with a loading force of 20 mN. The indentations are 2000 ± 6 nm ($N = 9$) in width and 170 ± 3 nm ($N = 9$) in depth. (b) A silver film (100 nm thick) with a 5 × 5 array of pyramids formed from the wafer in (a) upon template stripping. (c) A close-up high-resolution AFM image of a single pyramid on silver surface. (d) Raman scattering spectra for the same 4-methylbenzenethiol-coated pyramidal structure (at the tip) shown in (c) (green curve) and for neat 4-methylbenzenethiol (blue curve). The inset is an image acquired using a confocal Raman microscope with a wavelength of excitation of 633 nm. The image is the intensity of the signal at 1077 cm^{-1} (C−C symmetric stretching and C−S stretching).

DOI: 10.1021/nl101675s | *Nano Lett.* **2010,** *10,* 2702–2708

uniformly enhanced signals near the tip of a silver pyramid (inset of Figure 7d). Using a protocol reported previously,[28] we quantified the SERS enhancement by comparing the Raman signal from neat 4-methylbenzenethiol with that from our monolayer-coated pyramidal feature (Figure 7d). After correcting for the number of molecules, we determined an enhancement factor of 10^7-10^8 at the tip of the pyramidal structure.

Conclusions. Indentation lithography provides an inexpensive method for fabricating templates with arbitrary patterns of nano- and microscale features on a wide range of materials. Commercial indenter systems are available in materials science and engineering laboratories of many research universities. Rudimentary nanoindentation systems are sold by some manufacturers as "add-ons" to AFM systems. Indentation is, thus, becoming a ubiquitous tool.

Indentation lithography is part of a group of techniques that exploits the control and precision of analytical instruments for micro- and nanofabrication. In this sense, IndL is related to dip-pen nanolithography,[16] which uses an AFM to fabricate nanostructures, and nanoskiving,[29] which uses the diamond knife of an ultramicrotome. These techniques are capable of producing structures that are complementary to those produced by conventional methods of fabrication. As a purely mechanical technique, capable of applying very large or very small forces, IndL is unique in its insensitivity to the chemical properties of the substrate. It could, thus, be uniquely suited to mechanical patterning/machining of multilayered materials, delicate thin films, such as SAMs, and biological materials.

As with any technique, indentation lithography has limitations. Like conventional mastering techniques such as EBL, indentation lithography is serial and therefore its most promising applications are in mastering, rather than in replication, and in making unique structures for fundamental physical measurements. IndL tends to produce wide and shallow features. The exploration of custom-made indenter tips could enable the generation of high-aspect-ratio features. IndL is also slow, because the use of nanoindentation as a technique of measurement requires high sensitivity, rather than high speed. It might, however, be possible to fabricate arrays of diamond-tipped indenters for high-throughput patterning, in the same way that parallel dip-pen nanolithography[30] or IBM's Millipede[19] enables large-area patterning or data coding.

Acknowledgment. This work was supported by the National Science Foundation under award CHE-0518055. The authors used the shared facilities supported by the NSF under NSEC (PHY-0117795 and PHY-0646094) and MRSEC (DMR-0213805 and DMR-0820484). This work was performed in part using the facilities of the Center for Nanoscale Systems (CNS), a member of the National Nanotechnology Infrastructure Network (NNIN), which is supported by the National Science Foundation under NSF Award No. ECS-0335765. CNS is part of the Faculty of Arts and Sciences at Harvard University. D.J.L. acknowledges a graduate fellowship from the American Chemical Society, Division of Organic Chemistry, sponsored by Novartis. Z.H.N. acknowledges a postdoctoral fellowship from the Natural Science and Engineering Research Council of Canada. N.X.R. acknowledges Jim Gareau from Physik Instrumente for kindly loaning a displacement stage and controller.

Supporting Information Available. Details of experimental procedures, fabrication processes, and calculation of enhancement factors. This material is available free of charge via the Internet at http://pubs.acs.org.

REFERENCES AND NOTES

(1) Shir, D. J.; Jeon, S.; Liao, H.; Highland, M.; Cahill, D. G.; Su, M. F.; El-Kady, I. F.; Christodoulou, C. G.; Bogart, G. R.; Hamza, A. V.; Rogers, J. A. *J. Phys. Chem. B* **2007**, *111*, 12945–12958.
(2) Fischer-Cripps, A. C. *Nanoindentation*; Springer-Verlag: New York, 2002.
(3) Rosa, L. G.; Liang, J. *J. Phys.: Condens. Matter* **2009**, *21*, 18.
(4) Gates, B. D.; Xu, Q. B.; Stewart, M.; Ryan, D.; Willson, C. G.; Whitesides, G. M. *Chem. Rev.* **2005**, *105*, 1171–1196.
(5) Quake, S. R.; Scherer, A. *Science* **2000**, *290*, 1536–1540.
(6) Xia, Y. N.; Whitesides, G. M. *Annu. Rev. Mater. Sci.* **1998**, *28*, 153–184.
(7) Ruiz, S. A.; Chen, C. S. *Soft Matter* **2007**, *3*, 168–177.
(8) Bowen, A. M.; Nuzzo, R. G. *Adv. Funct. Mater.* **2009**, *19*, 3243–3253.
(9) Stewart, M.; Motala, M.; Yao, J.; Thompson, L.; Nuzzo, R. *Proc. Inst. Mech. Eng., IMechE Conf.* **2006**, *220*, 81–138.
(10) Xia, Y. N.; Tien, J.; Qin, D.; Whitesides, G. M. *Langmuir* **1996**, *12*, 4033–4038.
(11) Linder, V.; Wu, H. K.; Jiang, X. Y.; Whitesides, G. M. *Anal. Chem.* **2003**, *75*, 2522–2527.
(12) Craighead, H. G. *Science* **2000**, *290*, 1532–1535.
(13) Oliver, W. C.; Pharr, G. M. *J. Mater. Res.* **1992**, *7*, 1564–1583.
(14) Weiss, E. A.; Kaufman, G. K.; Kriebel, J. K.; Li, Z.; Schalek, R.; Whitesides, G. M. *Langmuir* **2007**, *23*, 9686–9694.
(15) Dinelli, F.; Menozzi, C.; Baschieri, P.; Facci, P.; Pingue, P. *Nanotechnology* **2010**, *21*, No. 075305.
(16) Piner, R. D.; Zhu, J.; Xu, F.; Hong, S. H.; Mirkin, C. A. *Science* **1999**, *283*, 661–663.
(17) Liu, G.-Y.; Xu, S.; Qian, Y. *Acc. Chem. Res.* **2000**, *33*, 457–466.
(18) Pires, D.; Hedrick, J. L.; De Silva, A.; Frommer, J.; Gotsmann, B.; Wolf, H.; Despont, M.; Duerig, U.; Knoll, A. W. *Science* **2010**, *328*, 732–735.
(19) Vettiger, P.; Cross, G.; Despont, M.; Drechsler, U.; Durig, U.; Gotsmann, B.; Haberle, W.; Lantz, M. A.; Rothuizen, H. E.; Stutz, R.; Binnig, G. K. *IEEE Trans. Nanotechnol.* **2002**, *1*, 39–55.
(20) Smith, R. K.; Lewis, P. A.; Weiss, P. S. *Prog. Surf. Sci.* **2004**, *75*, 1–68.
(21) Tseng, A. A.; Notargiacomo, A.; Chen, T. P. *J. Vac. Sci. Technol., B* **2005**, *23*, 877–894.
(22) Gwinner, M. C.; Koroknay, E.; Fu, L. W.; Patoka, P.; Kandulski, W.; Giersig, M.; Giessen, H. *Small* **2009**, *5*, 400–406.
(23) Oliver, W. C.; Pharr, G. M. *J. Mater. Res.* **2004**, *19*, 3–20.
(24) Xu, Q.; Mayers, B. T.; Lahav, M.; Vezenov, D. V.; Whitesides, G. M. *J. Am. Chem. Soc.* **2004**, *127*, 854–855.
(25) Nagpal, P.; Lindquist, N. C.; Oh, S.-H.; Norris, D. J. *Science* **2009**, *325*, 594–597.
(26) Haes, A. J.; Haynes, C. L.; McFarland, A. D.; Schatz, G. C.; Van Duyne, R. R.; Zou, S. L. *MRS Bull.* **2005**, *30*, 368–375.
(27) Campion, A.; Kambhampati, P. *Chem. Soc. Rev.* **1998**, *27*, 241–250.
(28) Bantz, K. C.; Haynes, C. L. *Langmuir* **2008**, *24*, 5862–5867.
(29) Xu, Q. B.; Rioux, R. M.; Dickey, M. D.; Whitesides, G. M. *Acc. Chem. Res.* **2008**, *41*, 1566–1577.
(30) Salaita, K.; Wang, Y. H.; Fragala, J.; Vega, R. A.; Liu, C.; Mirkin, C. A. *Angew. Chem., Int. Ed.* **2006**, *45*, 7220–7223.

DOI: 10.1021/nl101675s | *Nano Lett.* **2010,** *10,* 2702–2708